A Primer on Particle Sizing Using Dynamic Light Scattering

by Kevin Mattison, Ana Morfesis, and Michael Kaszuba

The efficacy and subsequent success of a pharmaceutical is strongly dependent on its shelf life and its stability under targeted solution conditions. A typical manifestation of formulation instability is an increase in particle size, due to aggregation of the analyte or carrier. As the particle size increases, efficacy is diminished, primarily due to the decrease in the active surface area. Because of the correlation between efficacy and size, particle sizing is quickly becoming a routine step in the development of more stable and effective formulations.

Dynamic light scattering (DLS), also known as photon correlation spectroscopy (PCS) and quasi-elastic light scattering (QELS), provides many advantages as a particle size analysis method. DLS is a noninvasive technique that measures a large population of particles in a very short time period, with no manipulation of the surrounding medium. Modern DLS instruments, notably the Zetasizer Nano system (Malvern Instruments, Southborough, MA), can measure particle sizes as small as 0.6 nm and as large as 6 µm across a wide range of sample concentrations. Because of the sensitivity to trace amounts of aggregates and the ability to resolve multiple particle sizes, DLS is ideally suited for macromolecular applications necessitating low sample concentration and volume, such as the development of stable food, drug, and surfactant formulations and in the screening of protein samples for crystallization trials.

Particles and macromolecules in solution undergo Brownian motion. Brownian motion arises from collisions between the particles and the solvent molecules. As a consequence of this particle motion, light scattered from the particle ensemble will fluctuate with time. In DLS, these fluctuations are measured across very short time intervals to produce a correlation curve, from which the particle diffusion coefficient (and subsequently the particle size) is extracted.

In contrast to separation techniques, where particles are separated and then counted, in the DLS technique, all of the size information for the ensemble of particles is contained within a single correlation curve. As such, particle size resolution requires a deconvolution of the data contained in the measured correlation curve. While standard algorithms exist for transforming the correlation curve to a particle size distribution, an understanding of the precision and accuracy of the distribution necessitates a solid understanding of the underlying principles behind the DLS technique itself. This article presents a brief overview of the DLS technique, along with common algorithms used to deconvolute the size distribution from the measured correlation curve.

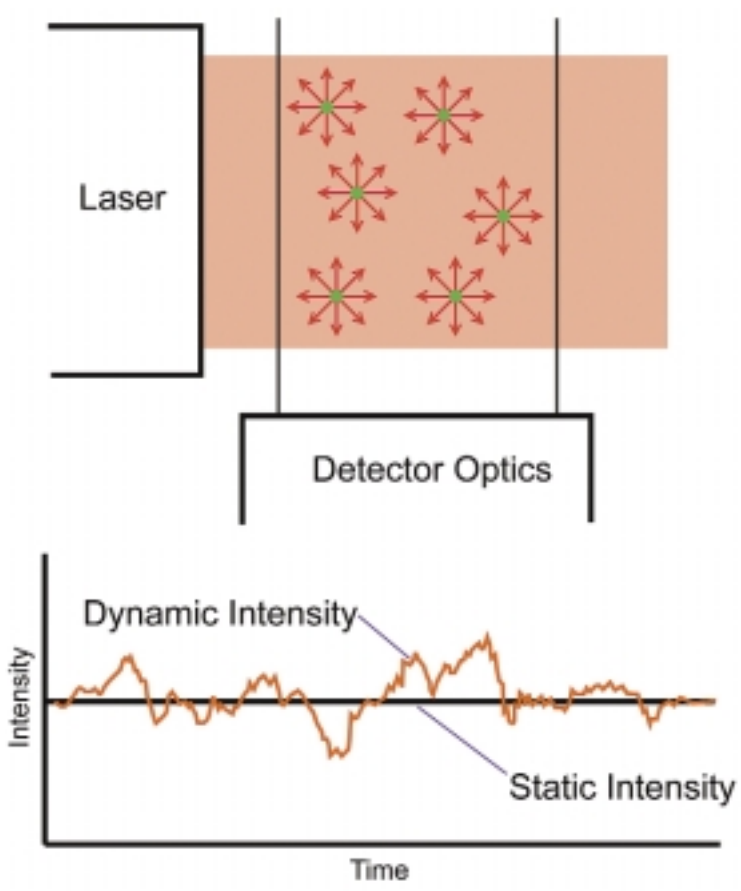

Figure 1 Schematic detailing the scattering volume and subsequent static and dynamic light scattering intensities.

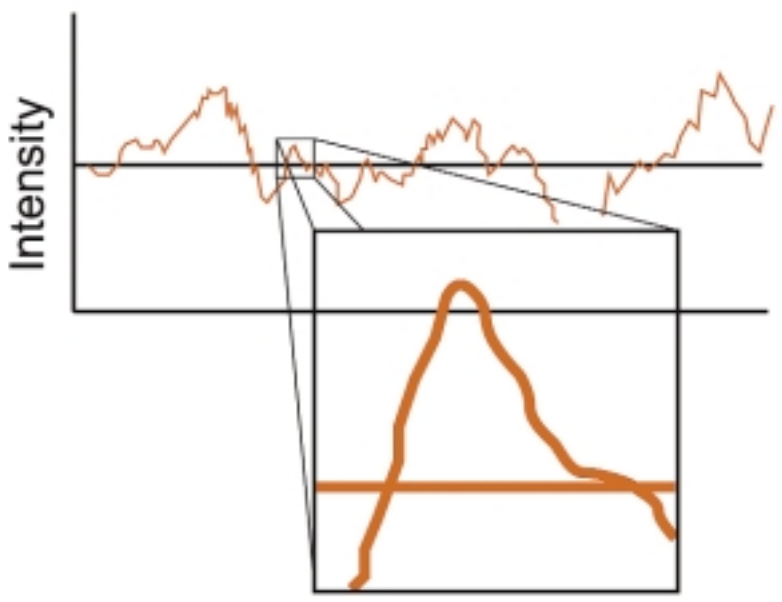

Figure 2 Intensity time trace showing the lack of discontinuity expected for a random signal when viewed across a short time interval.

Dynamic light scattering

Light scattering is a consequence of the interaction of light with the electric field of a particle or small molecule. This interaction induces a dipole in the particle electric field that oscillates with the same frequency as that of the incident light. Inherent to the oscillating dipole is the acceleration of charge, which leads to the release of energy in the form of scattered light.

For a collection of solution particles illuminated by a light source such as a laser, the scattering intensity measured by a detector located at some point in space will be dependent on the relative positions of the particles within the scattering volume. The scattering volume is defined as the crossover section of the light source and the detector optics. The position dependence of the scattering intensity arises from constructive and destruction interference of the scattered light waves. If the particles are static, or frozen in space, then one would expect to observe a scattering intensity that is constant with time, as described in *Figure 1*. In practice, however, the particles are diffusing according to Brownian motion, and the scattering intensity fluctuates about an average value equivalent to the static intensity. As detailed in Figure 1, these fluctuations are known as the dynamic intensity.

Across a long time interval, the dynamic signal appears to be representative of random fluctuations about a mean value. When viewed on a much smaller time scale, however (*Figure 2*), it is evident that the intensity trace is in fact not random, but rather comprises a series of continuous data points. This absence of discontinuity is a consequence of the physical confinement of the particles in a position very near to the position occupied a very short time earlier. In other words, on short time scales, the particles have had insufficient time to move very far from their initial positions, and as such, the intensity signals are very similar. The net result is an intensity trace that is smooth, rather than discontinuous.

Correlation is a second-order statistical technique for measuring the degree of nonrandomness in an apparently random data set. When applied to a time-dependent intensity trace, as measured with DLS instrumentation, the correlation coefficients, $G(\tau)$, are calculated as shown in Eq. (1), where t is the initial (start) time and τ is the delay time.

$$G(\tau) = \int_0^\infty I(t)I(t+\tau)dt \qquad (1)$$

As a summation, the correlation equation can be expressed as shown in Eq. (2), or expressed in a tabular format as shown in *Table 1*.

$$G_k(\tau_k) = \sum_{i=0} I(t_i)I(t_i+\tau_k) \qquad (2)$$

Typically, the correlation coefficients are normalized, such that $G(\infty) = 1$. For monochromatic laser light, this normalization imposes an upper correlation curve limit of 2 for $G(t_o)$ and a lower baseline limit of 1 for $G(\infty)$. In practice, however, the upper limit can only be achieved for carefully optimized optical systems. Typical experimental upper limits are approx. 1.8–1.9.

Table 1 Correlation coefficient equations for selected *k* index values

k	Intensity	Correlation coefficient
0	$I(t_0)$	
1	$I(t_1)$	$G_1(t_1) = I(t_0)I(t_1) + I(t_1)I(t_2) + I(t_2)I(t_3) + \ldots + I(t_{k-1})I(t_k)$
2	$I(t_2)$	$G_2(t_2) = I(t_0)I(t_2) + I(t_1)I(t_3) + I(t_2)I(t_4) + \ldots + I(t_{k-2})I(t_k)$
3	$I(t_3)$	$G_3(t_3) = I(t_0)I(t_3) + I(t_1)I(t_4) + I(t_2)I(t_5) + \ldots + I(t_{k-3})I(t_k)$
n	$I(t_n)$	$G_n(t_n) = I(t_0)I(t_n)$

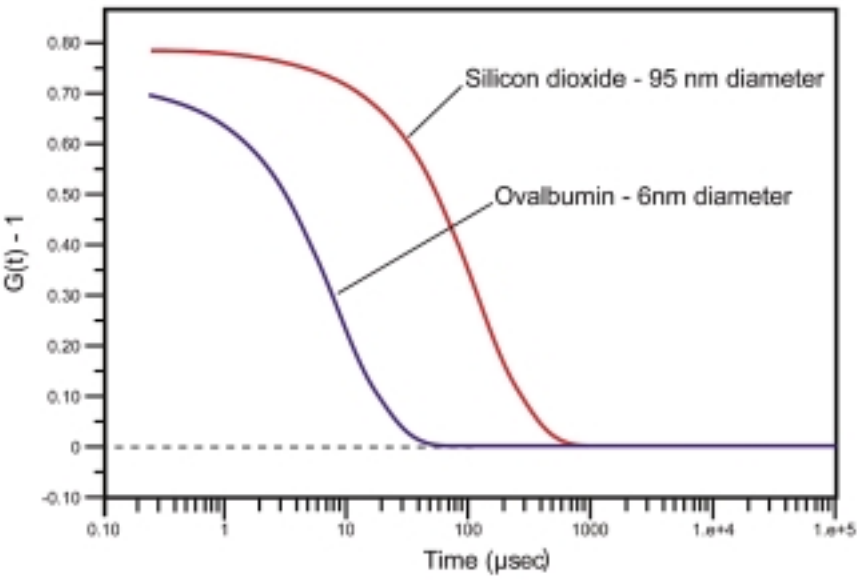

Figure 3 Intensity correlation curves for ovalbumin and silicon dioxide, measured with a Zetasizer Nano ZS static, dynamic, and electrophoretic light scattering instrument.

In DLS instrumentation, the correlation summations are performed using an integrated digital correlator, which is a logic board comprising operational amplifiers that continually add and multiply short time scale fluctuations in the measured scattering intensity to generate the correlation curve for the sample. Examples of correlation curves measured for two submicron particles are given in *Figure 3*. For the smaller and hence faster diffusing protein, the measured correlation curve has decayed to baseline within 100 µsec, while the larger and slower diffusing silicon dioxide particle requires nearly 1000 µsec before correlation in the signal is completely lost.

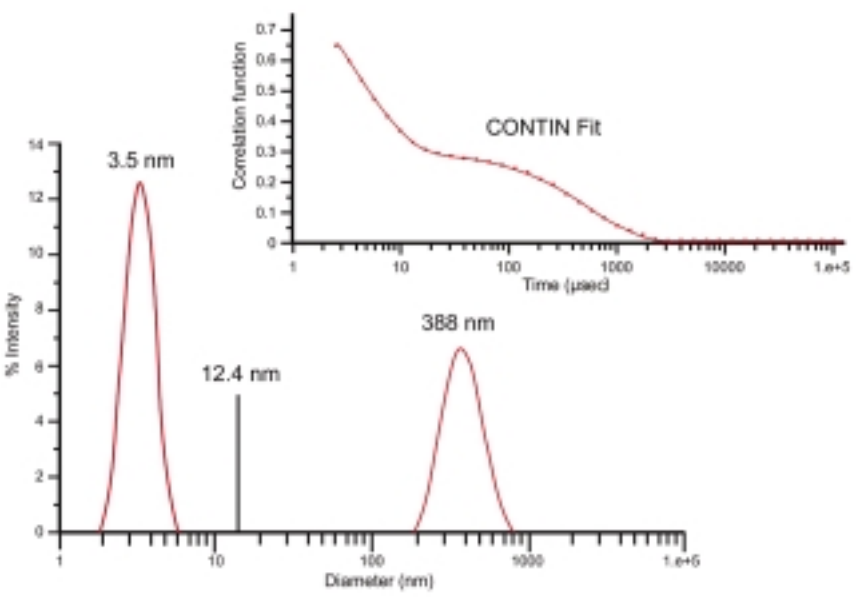

Figure 4 Correlation curve and CONTIN distribution for 10-mg/mL lysozyme in 100 mM NaCl at 69 °C, measured with a Zetasizer Nano ZS static, dynamic, and electrophoretic light scattering system. The Z average of 12.4 nm is indicated by the solid line in the distribution results.

Hydrodynamic size

All of the information regarding the motion or diffusion of the particles in the solution is embodied within the measured correlation curve. For monodisperse samples, consisting of a single particle size group, the correlation curve can be fit to a single exponential form as given in Eq. (3), where B is the baseline, A is the amplitude, and D is the diffusion coefficient. The scattering vector (q) is defined by Eq. (4), where $\tilde{n}$ is the solvent refractive index, λ_o is the vacuum wavelength of the laser, and θ is the scattering angle.

$$G(\tau) = \int_0^\infty I(t)I(t+\tau)dt = B + A\,e^{-2q^2D\tau} \qquad (3)$$

$$q = \frac{4\pi\tilde{n}}{\lambda_0}\sin\left(\frac{\theta}{2}\right) \qquad (4)$$

The hydrodynamic radius is defined as the radius of a hard sphere that diffuses at the same rate as the particle under examination. The hydrodynamic radius is calculated using the particle diffusion coefficient and the Stokes-Einstein equation given in Eq. (5), where k is the Boltzmann constant, T is the absolute temperature, and η is the solvent viscosity.

$$R_H = \frac{kT}{6\pi\eta D} \qquad (5)$$

A single exponential or Cumulant fit of the correlation curve is the fitting procedure recommended by the International Standards Organization (ISO). The hydrodynamic size extracted using this method is an average value, weighted by the particle scattering intensity. Because of the intensity weighting, the Cumulant size is defined as the Z average or intensity average.

While the Cumulant algorithm and the Z average are useful for describing general solution characteristics, for multimodal solutions, consisting of multiple particle size groups, the Z average can be misleading. For multimodal solutions, it is more appropriate to fit the correlation curve to a multiple exponential form, using common algorithms such as CONTIN or Non Negative Least Squares (NNLS). Consider, for example, the correlation curve shown in *Figure 4*. This correlation curve, measured for a 10-mg/mL lysozyme sample in 100 m*M* NaCl at 69 °C, clearly exhibits two exponential decays, one for the fast-moving monomer at 3.5 nm and one for the slow-moving aggregate at 388 nm. The size distribution shown in Figure 4 was derived using the CONTIN algorithm. When the single exponential Cumulant algorithm is used, a Z average of 12.4 nm is indicated, which is clearly inconsistent with the distribution results.

Figure 5 The Zetasizer Nano, a combined static, dynamic, and electrophoretic light scattering system.

System scope

The Zetasizer Nano system (*Figure 5*) includes the hardware and software for combined dynamic, static, and electrophoretic light scattering measurements, giving the researcher a wide range of sample properties, including the size, molecular weight, and zeta potential. The system was designed specifically to meet the low concentration and sample volume requirements typically associated with pharmaceutical and biomolecular applications, along with the high concentration requirements for colloidal

applications. Satisfying this unique mix of requirements was accomplished via the integration of a backscatter optical system and the design of a novel cell chamber. As a consequence of these features, the system specifications for sample size and concentration are noteworthy, with a size range of 0.6 nm to 6 µm and a concentration range of 0.1 mg/mL lysozyme to 40% wt/vol. Also, the Zetasizer hardware is self optimizing, and the software includes a "one click" measure, analyze, and report feature designed to minimize the new user learning curve.

Additional reading

Benight AS, Wilson DH, Budzynski DM, Goldstein RF. Dynamic light scattering investigations of RecA self-assembly and interactions with single strand DNA. Biochimie 1991; 73(2–3):143–55.

Brown RGW. Miniature laser light scattering instrumentation for particle size analysis. Appl Opt 1990; 29(28):1.

D'Arcy A. Crystallizing proteins—a rational approach. Acta Cryst 1994; D50:467–71.

Dynamic light scattering: applications of photon correlation spectroscopy. In: Pecora R, ed. Plenum Press, New York, 1985.

Fusett F, Dijkstra BW. Purification and light-scattering analysis of penicillin-binding protein 4 from Escherichia coli. *Microbiol Drug Res 1996; 2(1):73–6.*

Hutchinson FJ, Francis SE, Lyle IG, Jones MN. The characterization of liposomes with covalently attached proteins. Biochim Biophys Acta 1989; 978(1):17–24.

Moradian-Oldak J, Leung W, Fincham AG. Temperature and pH-dependent supramolecular self-assembly of amelogenin molecules: a dynamic light-scattering analysis. J Struct Biol 1998; 122(3):320–7.

Phillies GD. Quasielastic light scattering. Anal Chem 1990; 62(20):1049A–57A.

Piekenbrock T, Sackmann E. Quasielastic light scattering study of thermal excitations of F-actin solutions and of growth kinetics of actin filaments. Biopolymers 1992; 32(11): 1471–89.

Sam T, Pley C, Mandel M. A hydrodymanic study with quasi-elastic light scattering and sedimentation of bacterial elongation factor EF-Tu.guanosine-5′-diphosphate complex under nonassociating conditions. Biopolymers 1990; 30(3–4):299–308.

Santos NC, Sousa AMA, Betbeder D, Prieto M, Castanho MARB. Structural characterization of organized systems of polysaccharides and phospholipids by light scattering, spectroscopy, and electron microscopy. Carbohyd Res 1997; 300(1):31–40.

The authors are with **Malvern Instruments,** *10 Southville Rd., Southborough, MA 01772, U.S.A.; tel.: 508-480-0200; fax: 508-460-9692; e-mail: info@malvernusa.com; home page: www.malverninstruments.com.*